



## Excellent adsorption and desorption characteristics of polypyrrole/TiO<sub>2</sub> composite for Methylene Blue



Jingjing Li<sup>a</sup>, Jiangtao Feng<sup>a, \*\*</sup>, Wei Yan<sup>a,b,\*</sup>

<sup>a</sup> Department of Environmental Science and Engineering, Xi'an Jiaotong University, Xi'an 710049, PR China

<sup>b</sup> State Key Laboratory of Multiphase Flow in Power Engineering, Xi'an Jiaotong University, Xi'an 710049, PR China

### ARTICLE INFO

#### Article history:

Received 8 January 2013

Received in revised form 25 March 2013

Accepted 24 April 2013

Available online 2 May 2013

#### Keywords:

PPy  
PPy/TiO<sub>2</sub>  
Composite adsorbent  
Dye adsorption  
Regeneration

### ABSTRACT

P25 or self-prepared TiO<sub>2</sub> coated polypyrrole (PPy/P25 or PPy/TiO<sub>2</sub>) composites as novel adsorbents were prepared. Their adsorption–desorption characteristics for Methylene Blue (MB) were comparatively investigated. X-ray photoelectron spectroscopy (XPS) showed that PPy/TiO<sub>2</sub> possessed higher doping level than PPy/P25. Thermogravimetric analysis (TGA) indicated that PPy/TiO<sub>2</sub> contained more PPy than PPy/P25. The results of *water vapor adsorption* suggested that the PPy/TiO<sub>2</sub> composite was more hydrophobic than PPy/P25. The adsorption results revealed that the composites pretreated in the solution with higher pH value exhibited larger adsorption capacities. The ionic concentration in MB solution slightly impacted the removal of MB by the PPy/TiO<sub>2</sub> composite. The adsorption equilibrium results showed that the adsorption of MB was completed in a short time of 30 min. Pseudo-second-order and Langmuir isotherm models were effectively employed to describe the adsorption behavior of MB. PPy/TiO<sub>2</sub> and PPy/P25 were found to have better removal ability for MB compared with pure PPy; especially PPy/TiO<sub>2</sub>, on which the maximum adsorption amount was about 3.6 or 5.5 times higher than that of PPy/P25 or pure PPy, respectively. The thermodynamic analysis indicated that the adsorption of MB was spontaneous and endothermic in nature. The regeneration experiments exhibited that PPy/TiO<sub>2</sub> can be reused at least seven times without obvious loss of its original adsorption capacity. Electrostatic interaction, hydrogen bonding and hydrophobic interaction played the roles in MB adsorption performance. It is expected that the PPy/TiO<sub>2</sub> composite can be considered as a stable adsorbent for dye removal.

© 2013 Elsevier B.V. All rights reserved.

### 1. Introduction

The generated dye effluents from dye industries can cause serious water pollution problems if directly discharged into the environment. Therefore, it is important to remove dyes from dye wastewater. Recently, various treatment processes have been widely employed to remove dyes from wastewater [1]. In these methods, adsorption has been proved to be a reliable treatment approach due to its low capital investment, abundant raw material source, simple in design and operation, and non-toxic [2,3]. However, the choice of appropriate adsorbent for real applications is still a challenging issue. Although activated carbon is the present research focus, it also has many shortcomings, such as relative high cost of investment and operating, regeneration difficulty, and long time to adsorption equilibrium [4,5]. Therefore, the development of

new adsorbents with excellent adsorption and regeneration capacities becomes the research focus.

Polypyrrole (PPy) is one of the most commonly investigated conducting polymers owing to its non-toxic nature, environmental stability, low cost and simple preparation [6]. Because of the existed positively charged nitrogen atoms in PPy matrix, PPy possessed the adsorption ability through ion exchange or electrostatic interaction [6–8]. Moreover, PPy can undergo protonation or deprotonation processes when it is treated with acid or alkali solution, resulting in the change of its surface charges, followed by the doping or dedoping of counter ions [9,10]. Owing to the reversible transformation capability, PPy would have excellent regeneration ability, but this was rarely reported. Nevertheless, pure PPy showed a poor adsorption capacity [8,11]. Some publications have reported that the composites formed through PPy polymerizing on the surface of substrate materials can provide improved adsorption capacity, as compared with pure PPy [12,13]. Baumik et al. [12] prepared the PPy/Fe<sub>3</sub>O<sub>4</sub> magnetic composite and found that its maximum adsorption capacity for Cr(VI) could reach 169.4 mg/g at 25 °C. Lim et al. [13] fabricated PPy/silica nano-composite and testified that it could selectively adsorb Hg<sup>2+</sup> with the amount of 0.97 mmol/g.

\* Corresponding author at: State Key Laboratory of Multiphase Flow in Power Engineering, Xi'an Jiaotong University, Xi'an 710049, PR China.

\*\* Corresponding author. Tel.: +86 13891946894.

E-mail addresses: [fjtes@mail.xjtu.edu.cn](mailto:fjtes@mail.xjtu.edu.cn) (J. Feng), [yanwei@mail.xjtu.edu.cn](mailto:yanwei@mail.xjtu.edu.cn) (W. Yan).

However, the publications on the effect for the property of the selected substrate material on the adsorption capacity of composite were rarely reported. In this study, two kinds of titanium dioxide, the self-prepared TiO<sub>2</sub> (without calcination) and commercial P25, were chose as the substrate materials to synthesize the corresponding composite sorbents (PPy/TiO<sub>2</sub> or PPy/P25). Then their physicochemical properties and adsorption–desorption performances for Methylene Blue (MB, cationic dye) were studied. Pure PPy was also tested for comparison. In normal sol–gel processing, TiO<sub>2</sub> particles without calcination did not have complete crystallization and showed mainly amorphous. Zhang et al. [14] and Hoang et al. [15] indicated that the surface Ti atoms of the amorphous TiO<sub>2</sub> could not have full coordination, which existed in the forms of TiO<sub>5</sub> and TiO<sub>4</sub>. This resulted in more structure defects in the amorphous TiO<sub>2</sub>. Then the uncoordinated Ti atoms can act as active sites for chemical binding through ester-like linkage, bridging and chelating [14]. While P25 possessed complete and perfect crystallization, so its defects were relatively low. Therefore, the different nature of the amorphous TiO<sub>2</sub> and P25 may bring about the difference in the adsorption performance of the prepared PPy/TiO<sub>2</sub> and PPy/P25. The adsorption results exhibited that the PPy/TiO<sub>2</sub> and PPy/P25 composites possessed higher removal efficiencies than pure PPy. Moreover, the PPy/TiO<sub>2</sub> and PPy/P25 composites had different adsorption ability though they had a similar specific surface, and the adsorption amount of PPy/TiO<sub>2</sub> was nearly 3.6 times higher than that of PPy/P25. This suggested that the property of the selected substrate would severely impact the adsorption performance of the prepared composites. Additionally, the regeneration experiments indicated that the composites had the excellent adsorption stability.

## 2. Experimental

### 2.1. Materials

P25 powder (P25, Evonik Degussa) was purchased from Guangzhou HuaLiSen Trade Co., China. Pyrrole (98%, Qingquan Pharmaceutical & Chemical, Ltd., Zhejiang, China) was distilled twice under reduced pressure, and then stored in the dark under low temperature. Methylene Blue (MB) was purchased from Beijing Chemical Reagent Co., China. FeCl<sub>3</sub>·6H<sub>2</sub>O, CH<sub>3</sub>COOH, HNO<sub>3</sub> (65–68%), NaOH, n-propanol (99.9%) and tetrabutyl titanate (TBOT, 98%) were of analytical grade and used without further purification. The deionized water used for all experiments was obtained from the EPED-40TF Superpure Water System (EPED, China).

### 2.2. Synthesis of adsorbents

The preparation process of PPy/TiO<sub>2</sub> was described as follows. First, a mixture of TBOT and n-propanol with the volume ratio of 2.5:1 was added into 0.16 mol/L of HNO<sub>3</sub> solution (65 °C, 400 mL) with magnetic stirring for 2 h. A translucent TiO<sub>2</sub> solution was formed, followed by cooling down to ambient temperature. Then the TiO<sub>2</sub> solution was transferred to a 500 mL flask and cooled to 5 °C with mechanical stirring. Afterwards, pyrrole (0.25 mL) was added to the solution and stirred for 30 min, followed by adding dropwise FeCl<sub>3</sub> (1 mol/L, 10 mL) solution in 1 h. Then the mixture was reacted for additional 24 h statically. Finally the generated black solid was filtered and washed with deionized water several times, and then dried at 50 °C for 24 h. The solid was the PPy/TiO<sub>2</sub> composite.

For comparison, PPy/P25 was synthesized in the same recipe, except that the TiO<sub>2</sub> solution was replaced with P25 suspension (0.117 g/L). Pure PPy was synthesized in the same synthesis conditions except no P25 adding.

### 2.3. Characterization

X-ray diffraction (XRD) patterns were obtained with X'Pert PRO MRD diffractometer using Cu K $\alpha$  radiation. Raman spectra were recorded using Horiba HR800 Raman spectrophotometer. The BET surface area ( $S_{BET}$ ), total pore volume ( $V$ ) and average pore radius ( $R$ ) were measured at 77 K using Builder SSA-4200 (Beijing, China). The oxidative states of the samples were determined using X-ray photoelectron spectroscopy (XPS) on Kratos Axis Ultra DLD with an Al monochromatic X-ray source (1486.71 eV). All binding energies (BEs) were referenced to the C1s hydrocarbon peak at 284.6 eV. The thermogravimetric (TG) analyses were performed on Setaram Labsys Evo in N<sub>2</sub> flow and at a heating rate of 10 °C/min. The morphologies were characterized by scanning electron microscopy (SEM, JSM-6700F, Japan). The zeta potentials were measured with Malvern Zetasizer Nano ZS90. Samples for zeta potential measurement were prepared by adding 5 mg of composite in 10 mL NaCl solution (10<sup>-3</sup> mol/L) at different pH values (adjusted with diluted HNO<sub>3</sub> or NaOH solution).

Water vapor adsorption was regarded as a good means to evaluate the surface hydrophobicity of adsorbent. The adsorbent adsorbing a lower amount of water vapor was known to be more hydrophobic [16,17]. The process was similar to what was used by Wu et al. [17], except that the drying condition was 50 °C for 8 h, and the water vapor adsorption condition was 25 °C for 12 h.

### 2.4. Adsorption experiments

In order to study the influence of surface charge on the adsorption property, the adsorbents were pretreated with HNO<sub>3</sub> or NaOH solution (pH = 1.0–13.0, 5 mL). Then the pretreated adsorbents were centrifuged and used to conduct the MB solution without any processing (300 mg/L). The effect of ionic concentration (0–0.3 mol/L) on the adsorption was carried out by adding Na<sub>2</sub>SO<sub>4</sub> into the 300 mg/L MB solution.

All adsorption experiments were carried out in dark condition at 25 °C. The suspension containing 300 mg/L of MB solution and 2 g/L of adsorbent was stirred for 2 h. Then the suspension was centrifuged at 4000 rpm for 5 min. The supernatant was analyzed by the UV-vis spectrophotometer (Agilent 8453). The absorbance value of MB was read at the wavelength of 665 nm.

The adsorption rate  $R$  (%) and the amount of dye molecules adsorbed onto the adsorbents  $Q_t$  (mg/g) after the certain time  $t$  were calculated from Eqs. (1) and (2), respectively:

$$R = \frac{C_0 - C_t}{C_0} \times 100\% \quad (1)$$

$$Q_t = \frac{C_0 - C_t}{M} \times V \quad (2)$$

where  $C_0$  is the initial concentration (mg/L),  $C_t$  is the residual concentration at time  $t$  (mg/L),  $V$  is the solution volume (L), and  $M$  is the adsorbent mass (g).

The adsorption equilibrium of MB with different concentrations (200, 300 and 500 mg/L) on PPy/TiO<sub>2</sub> was evaluated at 25 °C, with 2 g/L of PPy/TiO<sub>2</sub> added and stirred for 2 h. The adsorption kinetics was investigated using the pseudo-first-order and pseudo-second-order models. Their linear forms are described in Eqs. (3) and (4), respectively:

$$\log(Q_{eq} - Q_t) = \log Q_{eq} - \frac{K_1}{2.303}t \quad (3)$$

$$\frac{t}{Q_t} = \frac{1}{K_2 Q_{eq}^2} + \frac{t}{Q_{eq}} \quad (4)$$

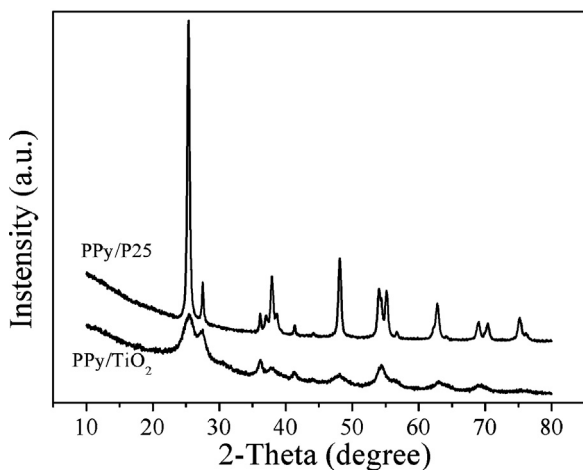


**Fig. 1.** XRD patterns of the PPy/P25 and PPy/TiO<sub>2</sub> composites.

where  $t$  is the adsorption time (min);  $K_1$  (1/min) and  $K_2$  (g/(mg min)) are the rate constants for the pseudo-first-order and pseudo-second-order models;  $Q_{eq}$  (mg/g) is adsorption amount at equilibrium state.

### 2.5. Adsorption isotherms

Adsorption isotherms of MB on PPy, PPy/TiO<sub>2</sub> and PPy/P25 at 25 °C were obtained by mixing different concentrations (50–700 mg/L) of MB solutions with 2 g/L of adsorbents. Langmuir and Freundlich isotherms are used to describe the adsorption behavior for MB, which are described in linear forms according to Eqs. (5) and (6), respectively:

$$\frac{C_{eq}}{Q_{eq}} = \frac{1}{Q_{max} K_L} + \frac{C_{eq}}{Q_{max}} \quad (5)$$

$$\ln Q_{eq} = \ln K_F + \frac{1}{n} \ln C_{eq} \quad (6)$$

where  $C_{eq}$  (mg/L) is the MB equilibrium concentration;  $Q_{max}$  (mg/g) is the maximum adsorption capacity;  $K_L$  (L/mg) is a constant that related to the heat of adsorption;  $K_F$  (mg/g) represents the adsorption capacity when  $C_{eq}$  equals 1;  $1/n$  represents the degree of dependence of adsorption on equilibrium concentration.

For thermomechanical analysis, the adsorption isotherm experiments were repeated in 15 and 35 °C.

### 2.6. Regeneration experiments

In order to test the regeneration ability, HNO<sub>3</sub> or CH<sub>3</sub>COOH solution ( $C = 1.0\text{--}0.01$  mol/L, 5 mL) was used to desorb MB adsorbed on the surface of PPy/TiO<sub>2</sub>. Then the desorbed PPy/TiO<sub>2</sub> was activated with 0.1 mol/L NaOH solution (5 mL). Finally the regenerated adsorbent was reused for the further adsorption experiments.

## 3. Results and discussion

### 3.1. Characterizations of the samples

**Fig. 1** shows the XRD patterns of PPy/P25 and PPy/TiO<sub>2</sub>. The results exhibited that PPy/P25 and PPy/TiO<sub>2</sub> were mixed crystals, for the characteristic diffraction peaks at 25.3° and 27.5° appeared in their patterns correspond well to the (101) plane of anatase TiO<sub>2</sub> and (110) plane of rutile TiO<sub>2</sub>, respectively. However, the peak intensity of PPy/TiO<sub>2</sub> is far weaker than that of PPy/P25, demonstrating that PPy/TiO<sub>2</sub> was mainly amorphous. It is also noted that

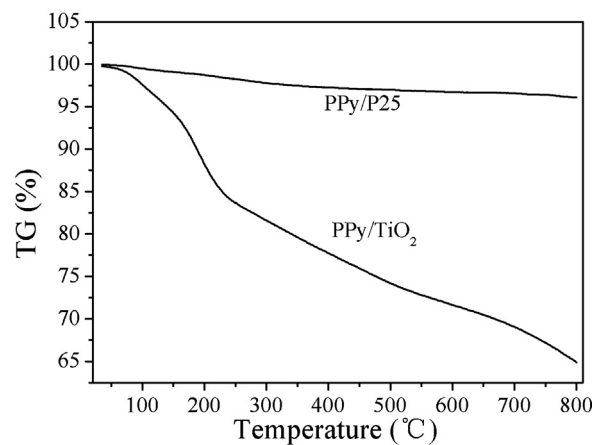


**Fig. 2.** TG analyses of the PPy/P25 and PPy/TiO<sub>2</sub> composites.

no new peaks appear in the patterns of PPy/TiO<sub>2</sub> and PPy/P25, which suggested that PPy was amorphous in the composite [18].

The TG analyses of PPy/P25 and PPy/TiO<sub>2</sub> are shown in **Fig. 2**. The first steep weight losses of about 6 wt% and 1 wt% before 150 °C for PPy/TiO<sub>2</sub> and PPy/P25, respectively, can be attributed to the adsorbed water [19]. Based on the TG analyses, the amount of PPy in the PPy/TiO<sub>2</sub> and PPy/P25 composites is approximately calculated to be about 20 wt% and 3 wt%, respectively, as the decomposition of PPy would happen between 150 and 500 °C [20]. This indicated that PPy/TiO<sub>2</sub> contained more PPy than PPy/P25. When the temperature exceeded 500 °C, the weight losses of PPy/TiO<sub>2</sub> and PPy/P25 were different. PPy/P25 nearly does not show a weight loss; while PPy/TiO<sub>2</sub> has about 10% weight loss, which may be due to the decomposition of NO<sub>3</sub><sup>-</sup> groups adsorbed on TiO<sub>2</sub> and the residual organics in self-prepared TiO<sub>2</sub>, and the dehydration of the hydrated TiO<sub>2</sub>.

**Fig. 3** shows the Raman spectra of PPy/P25 and PPy/TiO<sub>2</sub>. The double peaks at 1341 cm<sup>-1</sup> and 1546 cm<sup>-1</sup> for PPy/TiO<sub>2</sub>, 1345 cm<sup>-1</sup> and 1560 cm<sup>-1</sup> for PPy/P25 are assigned to the C=C backbone stretching and ring stretching of PPy, respectively [21]. Clearly, conjugated PPy was synthesized successfully. Meanwhile, the peaks of PPy/TiO<sub>2</sub> slightly shift to lower frequency, which suggested that PPy/TiO<sub>2</sub> had an increase in the conjugation length [21]. Besides, the bands of PPy/P25 at 142, 393, 445, 507 and 630 cm<sup>-1</sup> are the indication of P25 [22]. For PPy/TiO<sub>2</sub>, its bands at 139, 260, 413 and 598 cm<sup>-1</sup> have quite larger shifts, which deduced that PPy was chemisorbed on TiO<sub>2</sub> and the covalent-like binding was formed at

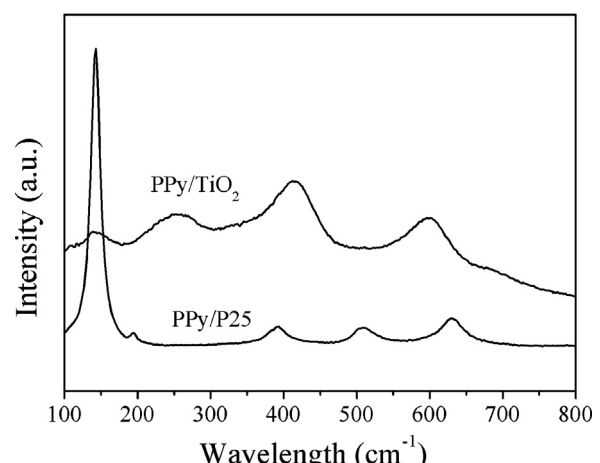


**Fig. 3.** Raman spectra of the PPy/P25 and PPy/TiO<sub>2</sub> composites.

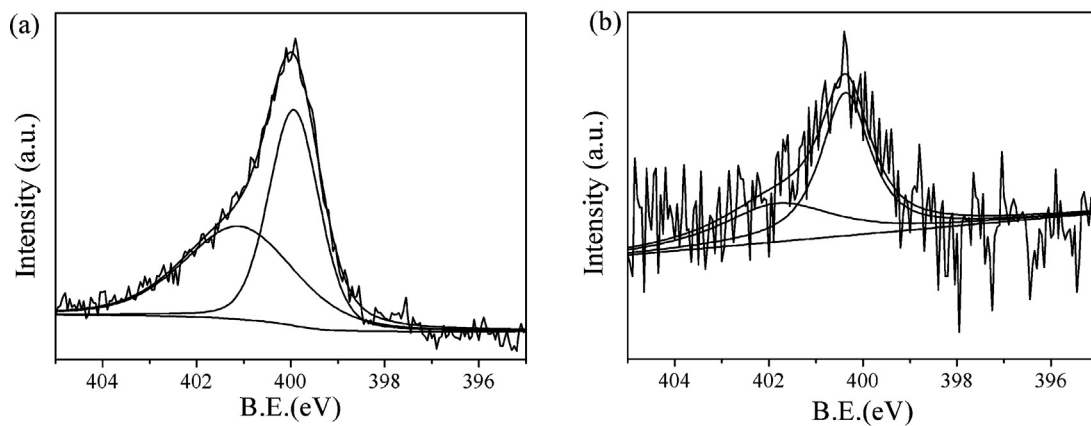


**Fig. 4.** XPS N1s core level spectra of the PPy/P25 and PPy/TiO<sub>2</sub> composites.

the interface [21,23]. Through the covalent-like binding between TiO<sub>2</sub> and PPy, PPy/TiO<sub>2</sub> showed more positively charged nitrogen atoms ( $-N^+$ ), which can be identified by the N 1s XPS spectra (as shown in Fig. 4). From the XPS spectra, the peaks at 399.9 and 401.3 eV are attributed to the neutral nitrogen atoms ( $-NH-$ ) and positively charged nitrogen atoms ( $-N^+$ ) in PPy layer, respectively. The proportions of  $-N^+$  in the PPy coating layers were found to be ca. 25% and 50% (in terms of  $N^+/N$ ) for PPy/P25 and PPy/TiO<sub>2</sub>, respectively. Some publications reported that the doping level ( $N^+/N$ ) of PPy prepared in Fe(III) salt was about 0.25–0.3 [10,24]. It was obvious that the doping level of PPy in PPy/TiO<sub>2</sub> was higher in this study, owing to the existence of a strong interaction between PPy and TiO<sub>2</sub>. The protonated nitrogen atoms contributed to the dye adsorption, resulting in PPy/TiO<sub>2</sub> containing more adsorption sites, followed by a higher adsorption capacity.

Fig. 5 shows the zeta potential values of PPy/P25 and PPy/TiO<sub>2</sub> as a function of the solution pH. The zeta potentials of PPy/P25 and PPy/TiO<sub>2</sub> are positive and remain relatively constant over the range of 3–9. Additionally, the isoelectric point ( $pH_{iep}$ ) of PPy/TiO<sub>2</sub> is slightly larger than that of PPy/P25, with the isoelectric points are about 10.5 and 10.3, respectively. Above the isoelectric point, the surface of adsorbent was negatively charged, and would be in favor of adsorbing cationic dye, MB.

The textural properties and the amount of water vapor adsorbed of PPy/TiO<sub>2</sub> and PPy/P25 are listed in Table 1. As observed, the  $S_{BET}$ , total pore volume and average pore radius of PPy/TiO<sub>2</sub> are smaller than that of PPy/P25, which may affect MB adsorption on PPy/TiO<sub>2</sub>. Besides, the amount of water vapor adsorbed on PPy/TiO<sub>2</sub> is lower

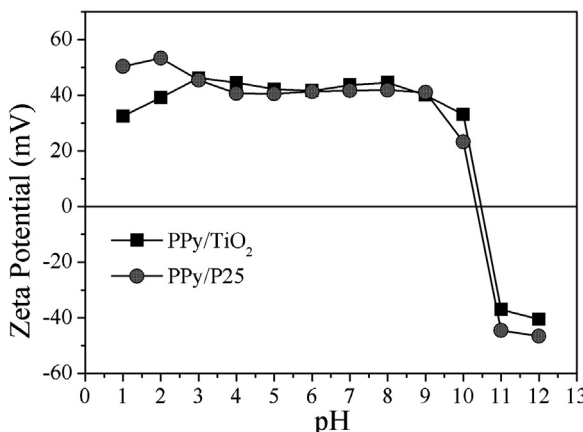


**Fig. 5.** Zeta potentials analyses of the PPy/P25 and PPy/TiO<sub>2</sub> composites.

**Table 1**  
Properties of different samples.

Samples	$S_{BET}$ (m <sup>2</sup> /g)	$V$ (cm <sup>3</sup> /g)	$R$ (nm)	Amount of water vapor adsorbed (%)
PPy/P25	56.31	0.36	10.70	17.20
PPy/TiO <sub>2</sub>	53.51	0.14	5.67	9.66

than that of PPy/P25. This showed that the PPy/TiO<sub>2</sub> was more hydrophobic than PPy/P25, which was in favor of the adsorption of MB on PPy/TiO<sub>2</sub>.

### 3.2. Adsorption experiments

#### 3.2.1. Effect of surface charge and ionic strength

The surface charge of adsorbent would be changed when it was pretreated with different treating agents (acid or alkali solution), which may affect its adsorption capacity, as shown in Fig. 6. The adsorption capacities of PPy/P25 and PPy/TiO<sub>2</sub> increase with the increasing pH of the treating agents and reach the largest adsorption amount at the pH of 13, indicating that MB could be easily absorbed onto the surface of the alkali-treated adsorbents. This was consistent with the zeta potentials analysis.

The publications suggested that the surface charge of PPy can be changed when it was immersed in acid or alkali solution [9,10]. Its

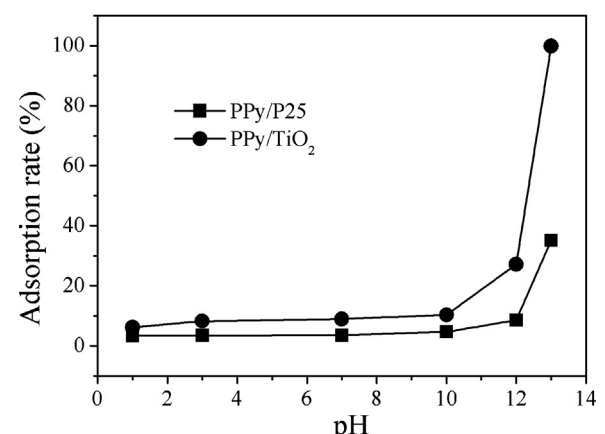


**Fig. 6.** Effect of surface charge on the adsorption capacities of the PPy/P25 and PPy/TiO<sub>2</sub> composites.

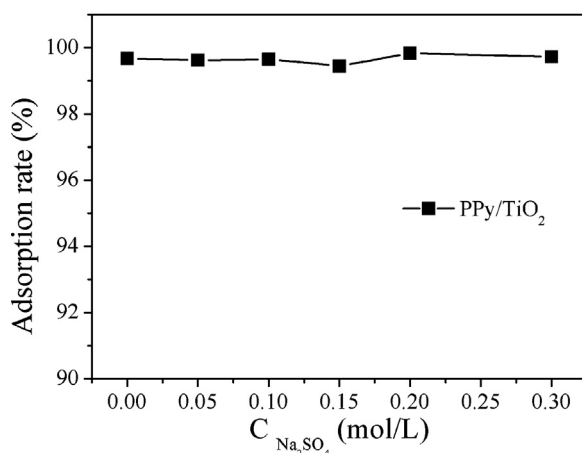
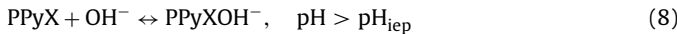
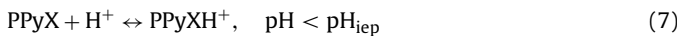


Fig. 7. Effect of ionic strength on the adsorption capacity of PPy/TiO<sub>2</sub>.

surface would be positively charged or negatively charged according to Eqs. (7) and (8):



where X is the counter anion. According to the results of zeta potential analyses, the surface of the adsorbents was negatively charged when the pH value of the treating agent was greater than 10.5. Thus, the cationic dye MB can be adsorbed on their surfaces through the electrostatic attraction. In contrast, the surface of the adsorbents was positively charged in the pH range of 1–10. Thereby, the composites exhibited poor removal efficiencies for MB due to the existence of the electrostatic repulsion. However, the composites still could adsorb MB. This was an indication that the electrostatic mechanism was not the only mechanism for dye adsorption in this system. PPy can also adsorb dye molecules via hydrogen bonding and hydrophobic mechanisms [8]. Nevertheless, the adsorption amount of MB in the pH range of 1–10 was far less than that in the pH range of 11–13, suggesting that the electrostatic interaction was the main mechanism. Moreover, the adsorption efficiency of PPy/TiO<sub>2</sub> was larger than that of PPy/P25, although the latter had better BET analysis results. However, PPy/TiO<sub>2</sub> contained more adsorption sites and was more hydrophobic. This implied that the adsorption capacity was controlled by several factors.

The effect of ionic concentrations on the adsorption performance is shown in Fig. 7. The results showed that the effect of the ionic concentration was unobvious. Zhang and Bai [7] indicated that the increase in ionic concentration reduced the electrostatic repulsion between the adsorbates, which would enhance the adsorption amount; however, it also weakened the electrostatic attraction between the adsorbates and adsorbents with the opposite charges, which can decrease the adsorption capacity. With the effects of the two aspects, the adsorption capacity of PPy/TiO<sub>2</sub> was almost not changed at the different ionic concentrations.

### 3.2.2. Adsorption isotherm

In order to describe the interaction between adsorbate and adsorbent, the equilibrium adsorption isotherm was investigated. Fig. 8 shows the linear forms of the Langmuir and Freundlich models for PPy, PPy/TiO<sub>2</sub> and PPy/P25. It is clearly observed that the degree of linearity of Langmuir model is better than that of Freundlich model. To be more specific, the experimental parameters of isotherm models are listed in Table 2. According to the correlation coefficients ( $R^2$ ), it was possible that the adsorption behaviors of the adsorbents were preferably described by the Langmuir model.

Moreover, the results of the error analyses are also displayed in Table 2. The standard error of estimate (SEE) is calculated according to Órfão et al. [25]. The isotherm model whose SSE value is smaller, suggesting it is more appropriate for describing the adsorption behavior. Obviously, the SSE value of Langmuir model is smaller than that of Freundlich model, indicating Langmuir model provided the better fit.

According to the Langmuir model, the maximum adsorption amounts of MB on PPy, PPy/P25 and PPy/TiO<sub>2</sub> were 49.72, 79.05 and 273.22 mg/g, respectively. It was clear that the composites possessed better adsorption performance than pure PPy, indicating the introduction of substrate material was effective. Moreover, PPy/TiO<sub>2</sub> exhibited better adsorption ability than PPy/P25, which implied that the properties of the substrate materials would affect the adsorption capacity of the prepared composites. From the XRD results, the PPy/TiO<sub>2</sub> composites were mainly amorphous; thus, TiO<sub>2</sub> in the PPy/TiO<sub>2</sub> composite possessed more defects than P25 in PPy/P25 [14,15]. This resulted in the formation of the covalent-like binding between PPy and TiO<sub>2</sub>, followed by the increased  $-\text{N}^+$  groups, and then the enhanced capacity. Table 3 lists the comparison of the adsorption capacity of PPy/TiO<sub>2</sub> with that of activated carbons previously investigated. It can be seen that the adsorption capacity of PPy/TiO<sub>2</sub> was not less than that of activated carbon. More importantly, PPy/TiO<sub>2</sub> had an obvious superiority that its equilibrium time was much shorter than that of activated carbon. This suggested that the PPy/TiO<sub>2</sub> adsorbent we prepared can be considered as a promising adsorbent for dye removal from wastewater.

Additionally, the adsorption isotherms of MB by PPy/TiO<sub>2</sub> at temperature of 15 °C and 35 °C were also studied. The calculated data are listed in Table 4. It was observed that the adsorption ability of PPy/TiO<sub>2</sub> increased with the rising temperature. This may be due to an increase in thermal energy of the adsorption species which led to higher adsorption capacity [12]. This indicated that MB adsorption by PPy/TiO<sub>2</sub> was endothermic in nature.

### 3.2.3. Thermodynamic study

The thermodynamic parameters such as changes in standard Gibbs free energy ( $\Delta G^\circ$ ), entropy ( $\Delta S^\circ$ ) and enthalpy ( $\Delta H^\circ$ ) for the adsorption of MB by PPy/TiO<sub>2</sub> were determined by using Eqs. (9) and (10):

$$\ln K_L = \frac{\Delta S^\circ}{R} + \frac{-\Delta H^\circ}{RT} \quad (9)$$

$$\Delta G^\circ = -RT \ln K_L \quad (10)$$

where  $R$  (kJ/(mol K)) is the gas constant and  $T$ (K) is the temperature.  $K_L$  (L/mg) is the constant of the Langmuir model. The related parameters were calculated and listed in Table 4. The positive value of  $\Delta H^\circ$  indicated that the process was endothermic in nature, while the positive value of  $\Delta S^\circ$  suggested that an increase in disorder at the solid-solution interface during the adsorption of dye. The decrease in  $\Delta G^\circ$  values with the increasing temperature determined that the adsorption process was spontaneous.

### 3.2.4. Adsorption kinetics

Apart from possessing a high adsorption capacity, it is essential for an adsorbent to exhibit rapid adsorption kinetics in removing adsorbate from solution. Fig. 9a represents the influences of contact time and initial concentration on the adsorbed MB on PPy/TiO<sub>2</sub>. It is obvious that MB uptake was rapid and a minimum contact time was sufficient enough for the removal of MB from water. Therefore, it is feasible that 2 h was chosen as the adsorption time in the following adsorption experiments. In addition, the adsorption amount increased with the increase in the initial concentration.

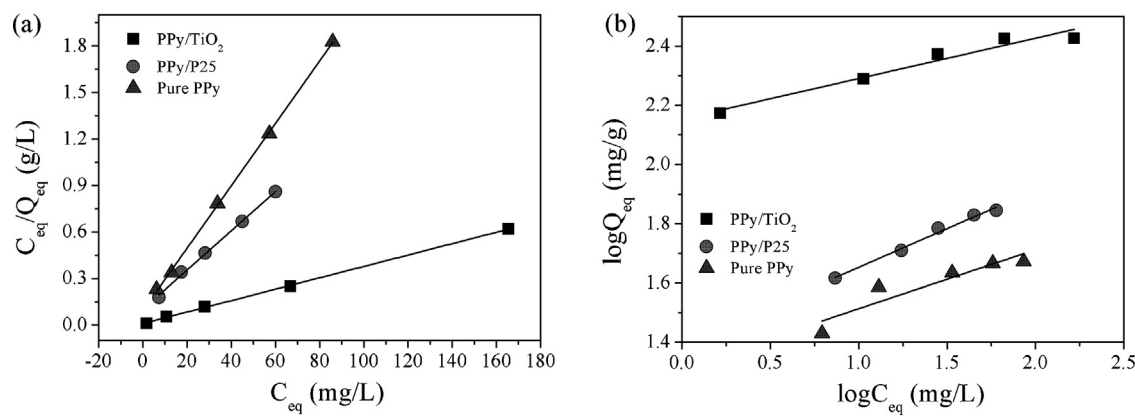


**Fig. 8.** Adsorption isotherm of MB on pure PPy, PPy/P25 and PPy/TiO<sub>2</sub>, the linear forms for (a) Langmuir isotherm model and (b) Freundlich isotherm model.

**Table 2**

Parameters of Langmuir and Freundlich adsorption isotherm models at 25 °C.

Adsorbent	Langmuir model				Freundlich model			
	Q <sub>max</sub> (mg/g)	K <sub>L</sub> (L/mg)	R <sup>2</sup>	SSE (mg/g)	K <sub>F</sub> (mg/g)	n	R <sup>2</sup>	SSE (mg/g)
PPy	49.72 ± 1.45	0.22 ± 0.02	0.999	1.45	20.75 ± 3.14	5.20 ± 1.46	0.827	3.47
PPy/P25	79.05 ± 3.27	0.13 ± 0.01	0.997	2.63	24.67 ± 1.31	3.84 ± 0.24	0.985	1.70
PPy/TiO <sub>2</sub>	273.22 ± 3.90	0.26 ± 0.08	0.999	6.23	152.77 ± 14.00	8.50 ± 1.73	0.870	12.49

**Table 3**

Comparison of the adsorption properties of different adsorbents for MB.

Adsorbents	Q <sub>max</sub> (mg/g)	Equilibrium time (h)	References
PPy/TiO <sub>2</sub>	273.22	0.5	This work
Bamboo-based activated carbon	454	48	[26]
Activated carbon	270	>400	[27]
Rattan sawdust-activated carbon	294.12	24	[28]
Activated carbon from oil palm wood	90.9	—	[29]
Bamboo-based activated carbon	183.3–286.1	24	[30]

**Table 4**

Thermodynamic and Langmuir parameters for MB adsorption on PPy/TiO<sub>2</sub> at different temperature.

Temperature (K)	Q <sub>max</sub>	K <sub>L</sub> (L/mg)	ΔG° (kJ/mol)	ΔS° (J/(mol K))	ΔH° (kJ/mol)
288	250.62	0.090	−8.05		
298	273.22	0.29	−11.23	223.39	
308	298.50	0.41	−12.48		55.98

**Table 5**

Parameters of the pseudo-first-order and pseudo-second-order models.

C <sub>0</sub> (mg/L)	Pseudo-first-order model				Pseudo-second-order model		
	Q <sub>eq</sub> <sup>a</sup> (mg/g)	K <sub>1</sub> (1/min)	Q <sub>eq</sub> <sup>b</sup> (mg/g)	R <sup>2</sup>	K <sub>2</sub> (g/(mg min))	Q <sub>eq</sub> <sup>b</sup> (mg/g)	R <sup>2</sup>
200	99.74	0.14	0.97	0.5328	2.79	99.70	1.00
300	149.57	0.12	49.60	0.8231	0.010	150.37	0.9999
500	238.56	0.11	86.08	0.8419	0.0054	240.38	0.9999

<sup>a</sup> Q<sub>eq</sub> is from the experimental measurement.

<sup>b</sup> Q<sub>eq</sub> is calculated from the kinetics model.

**Fig. 9b** and **c** is the kinetics curves of PPy/TiO<sub>2</sub>, and the related parameters are calculated and listed in **Table 5**. According to the values of the correlation coefficients, the pseudo-second-order model ( $R^2 = 0.9999\text{--}1.0$ ) was more appropriate for describing the adsorption behavior of MB. Furthermore, the calculated values of Q<sub>eq</sub> from the pseudo-second-order model approximately equaled to the experimentally obtained values. Besides, the rate constant decreases with the increase in the initial concentration of MB, suggesting that it needed a longer time to adsorption equilibrium at a higher initial concentration (as shown in **Fig. 9a**). It was probably because there was an electrostatic repulsion between the adsorbed

and free MB molecules hindering the transport of the free MB from the bulk solution to the surface of PPy/TiO<sub>2</sub> [7].

### 3.3. Regeneration experiments

Based on the effect of surface charge on the adsorption, it was feasible that the acid solution can be employed to realize desorption of the adsorbed MB. Two kinds of acid solutions with different concentrations (0.01–1.0 mol/L), HNO<sub>3</sub> or CH<sub>3</sub>COOH, were employed to investigated the desorption performance, as shown in **Table 6**. It was noted that the desorption efficiencies rose with the increase

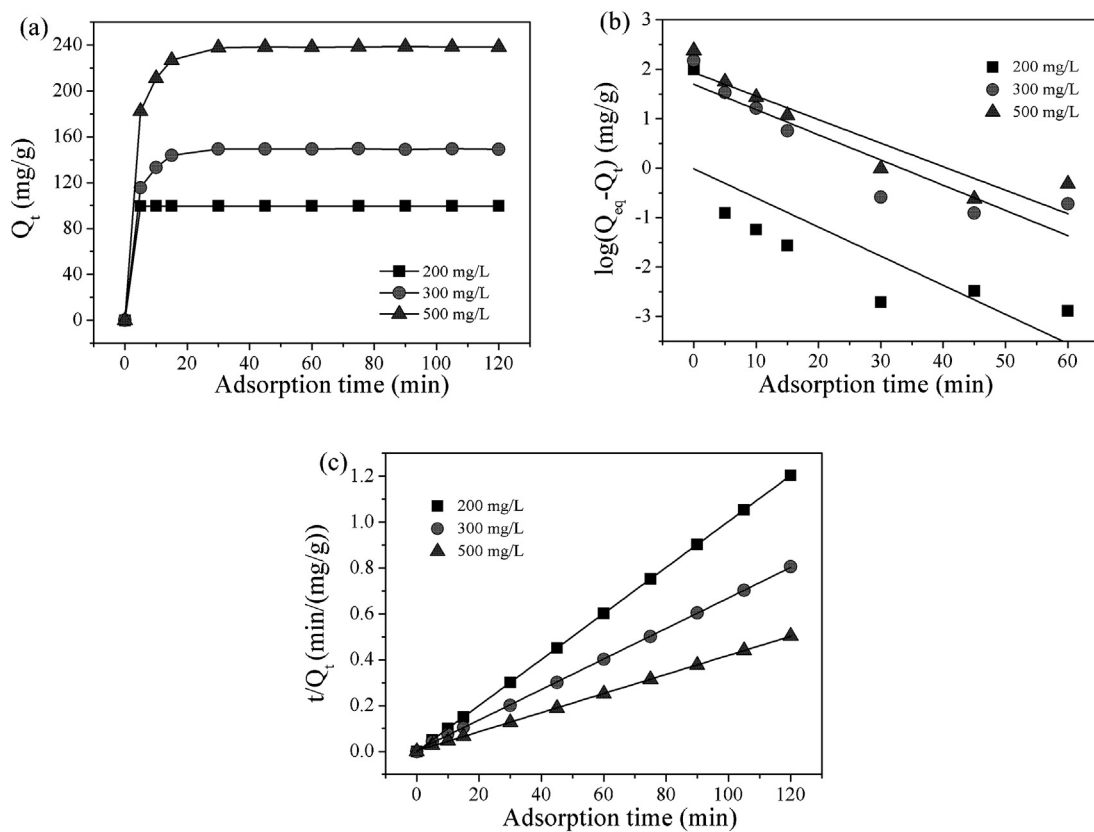


**Fig. 9.** Adsorption performance of PPy/TiO<sub>2</sub> for MB with different concentrations: (a) adsorption equilibrium curves of MB; (b) pseudo-first-order kinetic plots for the adsorption of MB; (c) pseudo-second-order kinetic plots for the adsorption of MB.

of the acid concentration due to the enhanced electrostatic repulsion. Besides, the desorption efficiency of CH<sub>3</sub>COOH solution was better than that of HNO<sub>3</sub> under the same concentration. This can be explained by using the similar compatible principle. Consequently, CH<sub>3</sub>COOH solution (1.0 mol/L) was available for desorption of MB, with the desorption efficiency of 81.63%.

The desorbed PPy/TiO<sub>2</sub> was activated with 0.1 mol/L NaOH solution. Afterwards, the regenerated PPy/TiO<sub>2</sub> was utilized to adsorb the same concentration of MB in order to study its adsorption stability. Fig. 10 shows the adsorption stability of PPy/TiO<sub>2</sub>. It can be seen that the adsorption capacity of PPy/TiO<sub>2</sub> is still higher than 93% after regeneration for seven times, indicating that this composite possessed excellent adsorption capacity and stability. The slight decrease of the adsorption capacity may be attributed to the incomplete desorption of MB adsorbed on PPy/TiO<sub>2</sub>. Compared with activated carbon, PPy/TiO<sub>2</sub> exhibited a comparable

regeneration property, as shown in Table 6. These results demonstrated that the PPy/TiO<sub>2</sub> adsorbent we prepared possessed better regeneration ability.

### 3.4. Adsorption mechanism

It was essential to understand the adsorption mechanism for a good adsorbent. Surface charge of adsorbent played an important role in adsorption. The adsorption capacity of PPy/TiO<sub>2</sub> was varied with its surface charge. When the pH value of the treating agent was greater than the  $pH_{iep}$  of PPy/TiO<sub>2</sub>, its surface would carry negative charges. Then, it could adsorb cationic dye MB through the electrostatic attraction. On the contrary, it would be positively charged when the pH value of the treating agent was lower than the  $pH_{iep}$ , followed by the inhibited adsorption ability due to the existence of electrostatic repulsion. This confirmed that the

**Table 6**  
Comparison of the desorption properties of different adsorbents.

Adsorbents	Adsorbates	Desorption agent	DE (%)	References
PPy/TiO <sub>2</sub>	MB	0.01 mol/L CH <sub>3</sub> COOH	54.26	This work
		0.1 mol/L CH <sub>3</sub> COOH	66.18	
		1.0 mol/L CH <sub>3</sub> COOH	81.63	
		0.01 mol/L HNO <sub>3</sub>	20.51	
		0.1 mol/L HNO <sub>3</sub>	25.94	
		1.0 mol/L HNO <sub>3</sub>	32.09	
Activated carbon from waste tires	Red 31	Ethanol	30–40%	[5]
	Black 5	Ethanol	40–50%	
Coconut shell granular activated carbon	Peach red	60% acetone	58%	[31]
	Mustard yellow	40% isopropanol	88%	
Commercial activated carbon	Congo Red	KOH	32.5%	[32]
		Surfactant	65%	

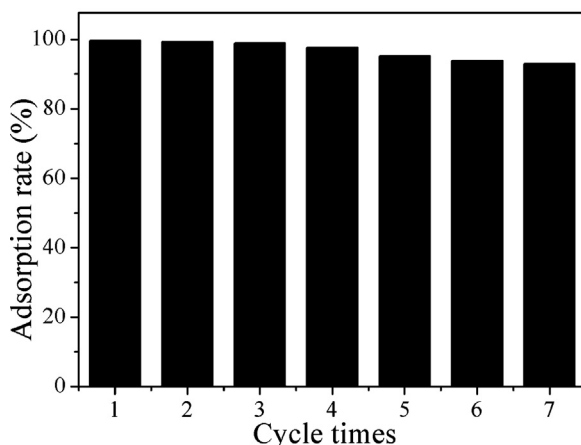


Fig. 10. The adsorption stability of PPy/TiO<sub>2</sub> for 300 mg/L of MB.

electrostatic interaction was the main adsorption force. However, it was also observed that PPy/TiO<sub>2</sub> still adsorbed MB when the pH value of the treating agent was lower than the pH<sub>iep</sub>, which indicated that the hydrogen bonding was another adsorption mechanism. The poor removal efficiency suggested that hydrogen bonding was not as significant as the electrostatic interaction. Besides, the water vapor adsorption experiments confirmed that PPy/TiO<sub>2</sub> was more hydrophobic than PPy/P25. Since the MB adsorption results demonstrated that PPy/TiO<sub>2</sub> possessed a higher adsorption capacity than PPy/P25. This suggested that the hydrophobic interaction was also the adsorption mechanism for MB adsorption. Therefore, the electrostatic interaction, hydrogen bonding and hydrophobic interaction played the roles in MB adsorption together, and the electrostatic interaction played the major role.

#### 4. Conclusions

In this paper, the PPy/TiO<sub>2</sub> and PPy/P25 composites were synthesized, characterized and compared to studying the adsorption performance for MB. The substrate material (P25 or self-prepared TiO<sub>2</sub>) seriously affected the physicochemical properties and adsorption capacities of the corresponding PPy/P25 or PPy/TiO<sub>2</sub>. The results of XRD patterns indicated that they have different crystal form and crystallinity. Raman analyses suggested that PPy was chemisorbed to TiO<sub>2</sub> with the formation of a covalent-like binding. TGA results indicated that PPy/TiO<sub>2</sub> contained more PPy than PPy/P25. XPS analyses exhibited that the amount of the  $-N^+$ -atoms for PPy/TiO<sub>2</sub> was twice as large as that for PPy/P25. The adsorption results indicated that the surface charge of composites was impacted by the pH values of the treating agents, followed by affecting the removal efficiency of MB. The largest efficiency was reached when the pH value of the treating agent was 13.0. MB adsorption was rapid and it could reach equilibrium in a short time of 30 min. Its adsorption behavior was well described by the pseudo-second-order model and Langmuir isotherm model. The calculated maximum adsorption amounts of PPy/TiO<sub>2</sub> and PPy/P25 were larger than that of pure PPy; especially PPy/TiO<sub>2</sub>, its maximum adsorption amount was about 3.6 or 5.5 times higher than that of PPy/P25 or pure PPy, respectively. The thermodynamic analysis indicated that the adsorption of MB was spontaneous and endothermic in nature. Desorption studies revealed that 1.0 mol/L CH<sub>3</sub>COOH was an appropriate desorption agent. After activated with 0.1 mol/L NaOH solution, PPy/TiO<sub>2</sub> could be reused for six times without appreciable loss of its original capacity. Electrostatic interaction, hydrogen bonding and hydrophobic interaction played the roles in MB adsorption performance. We believe that

the PPy/TiO<sub>2</sub> composite is a promising adsorbent in the removal of cationic dye from the wastewater, by comparing its adsorption equilibrium time, adsorption and regeneration capacities with that of activated carbon.

#### Acknowledgments

The authors gratefully acknowledge the financial supports from the Fundamental Research Funds for the Central Universities of China, the Specialized Research Fund for the Doctoral Program of Higher Education of China (20090201110005) and the Natural science fund of Jiangsu Province of China (SBK201022919).

#### References

- [1] E. Forgacs, T. Cserháti, G. Oros, Removal of synthetic dyes from wastewaters: a review, *Environment International* 30 (2004) 953–971.
- [2] Ö. Gerçel, A. Özcan, A.S. Özcan, H.F. Gerçel, Preparation of activated carbon from a renewable bio-plant of *Euphorbia rigida* by H<sub>2</sub>SO<sub>4</sub> activation and its adsorption behavior in aqueous solutions, *Applied Surface Science* 253 (2007) 4843–4852.
- [3] V. Belessi, G. Romanosa, N. Boukosa, D. Lambropouloud, C. Trapalis, Removal of Reactive Red 195 from aqueous solutions by adsorption on the surface of TiO<sub>2</sub> nanoparticles, *Journal of Hazardous Materials* 170 (2009) 836–844.
- [4] P.C.C. Faria, J.J.M. Órfão, M.F.R. Pereira, Adsorption of anionic and cationic dyes on activated carbons with different surface chemistries, *Water Research* 38 (2004) 2043–2052.
- [5] W. Tanthapanichakoon, P. Ariyadejwanich, P. Japthong, K. Nakagawa, S.R. Mukai, H. Tamon, Adsorption–desorption characteristics of phenol and reactive dyes from aqueous solution on mesoporous activated carbon prepared from waste tires, *Water Research* 39 (2005) 1347–1353.
- [6] N. Ballav, A. Maity, S.B. Mishra, High efficient removal of chromium(VI) using glycine doped polypyrrole adsorbent from aqueous solution, *Chemical Engineering Journal* 198 (2012) 536–546.
- [7] X. Zhang, R.B. Bai, Adsorption behavior of humic acid onto polypyrrole-coated nylon 6,6 granules, *Journal of Materials Chemistry* 12 (2002) 2733–2739.
- [8] X. Zhang, R.B. Bai, Y.W. Tong, Selective adsorption behaviors of proteins on polypyrrole-based adsorbents, *Separation and Purification Technology* 52 (2006) 161–169.
- [9] Q.B. Pei, R.Y. Qian, Protonation and deprotonation of polypyrrole chain in aqueous solutions, *Synthetic Metals* 45 (1991) 35–48.
- [10] X. Zhang, R.B. Bai, Surface electric properties of polypyrrole in aqueous solutions, *Langmuir* 19 (2003) 10703–10709.
- [11] M. Karthikeyan, K.K. Satheeshkumar, K.P. Elango, Removal of fluoride ions from aqueous solution by conducting polypyrrole, *Journal of Hazardous Materials* 167 (2009) 300–305.
- [12] M. Baumik, A. Maity, V.V. Srinivasu, M.S. Onyang, Enhanced removal of Cr(VI) from aqueous solution using polypyrrole/Fe<sub>3</sub>O<sub>4</sub> magnetic nanocomposite, *Journal of Hazardous Materials* 190 (2011) 381–390.
- [13] C.W. Lim, K. Song, S.H. Kim, Synthesis of PPy/silica nanocomposites with cratered surfaces and their application in heavy metal extraction, *Journal of Industrial and Engineering Chemistry* 18 (2012) 24–28.
- [14] Q.L. Zhang, L.C. Du, Y.X. Weng, L. Wang, H.Y. Chen, J.Q. Li, Particle-size-dependent distribution of carboxylate adsorption sites on TiO<sub>2</sub> nanoparticle surfaces: insights into the surface modification of nanostructured TiO<sub>2</sub> electrodes, *Journal of Physical Chemistry B* 108 (2004) 15077–15083.
- [15] V.V. Hoang, H. Zung, N.H.B. Trong, Structural properties of amorphous TiO<sub>2</sub> nanoparticles, *European Physical Journal D* 44 (2007) 515–524.
- [16] X.S. Zhao, G.Q. Lu, X. Hu, Characterization of the structural and surface properties of chemically modified MCM-41 material, *Microporous Mesoporous Mater.* 41 (2000) 37–47.
- [17] Z.J. Wu, I.S. Ahn, C.H. Lee, J.H. Kim, Y.G. Shul, K. Lee, Enhancing the organic dye adsorption on porous xerogels, *Colloids and Surfaces A: Physicochemical and Engineering Aspects* 240 (2004) 157–164.
- [18] D.S. Wang, Y.H. Wang, X.Y. Li, Q.Z. Luo, J. An, J.X. Yue, Sunlight photocatalytic activity of polypyrrole–TiO<sub>2</sub> nanocomposites prepared by ‘in situ’ method, *Catalysis Communications* 9 (2008) 1162–1166.
- [19] C. Lai, G.R. Li, Y.Y. Dou, X.P. Gao, Mesoporous polyaniiline or polypyrrole/anatase TiO<sub>2</sub> nanocomposites as anode materials for lithium-ion batteries, *Electrochimica Acta* 55 (2010) 4567–4572.
- [20] M. Omastová, M. Trchová, J. Kovářová, J. Stejskal, Synthesis and structural study of polypyroles prepared in the presence of surfactants, *Synthetic Metals* 138 (2003) 447–455.
- [21] J. Wang, X.Y. Ni, Photoresponsive polypyrrole–TiO<sub>2</sub> nanoparticles film fabricated by a novel surface initiated polymerization, *Solid State Communications* 146 (2008) 239–244.
- [22] I.M. Arabatzis, S. Antonaraki, T. Stergiopoulos, A. Hiskia, E. Papaconstantinou, M.C. Bernard, P. Falaras, Preparation, characterization and photocatalytic activity of nanocrystalline thin film TiO<sub>2</sub> catalysts towards 3,5-dichlorophenol degradation, *Journal of Photochemistry and Photobiology A: Chemistry* 149 (2002) 237–245.

- [23] Z. Weng, X.Y. Ni, Oxidative polymerization of pyrrole photocatalyzed by TiO<sub>2</sub> nanoparticles and interactions in the composites, *Journal of Applied Polymer Science* 110 (2008) 109–116.
- [24] E.T. Kang, K.G. Neoh, Y.K. Ong, K.L. Tan, B.T.G. Tan, X-ray photoelectron spectroscopic studies of polypyrrole synthesized with oxidative Fe(III) salts, *Macromolecules* 24 (1991) 2822–2828.
- [25] J.J.M. Órfão, A.I.M. Silva, J.C.V. Pereira, S.A. Barata, I.M. Fonseca, P.C.C. Faria, M.F.R. Pereira, Adsorption of a reactive dye on chemically modified activated carbons—Influence of pH, *Journal of Colloid and Interface Science* 296 (2006) 480–489.
- [26] B.H. Hameed, A.L. Ahmad, A.T.M. Din, Adsorption of methylene blue onto bamboo-based activated carbon: kinetics and equilibrium studies, *Journal of Hazardous Materials* 141 (2007) 819–825.
- [27] S.B. Wang, Z.H. Zhu, Effects of acidic treatment of activated carbons on dye adsorption, *Dyes and Pigments* 75 (2007) 306–314.
- [28] B.H. Hameed, A.L. Ahmad, K.N.A. Latiff, Adsorption of basic dye (Methylene Blue) onto activated carbon prepared from rattan sawdust, *Dyes and Pigments* 75 (2007) 143–149.
- [29] A.L. Ahmad, M.M. Loh, J.A. Aziz, Preparation and characterization of activated carbon from oil palm wood and its evaluation on Methylene Blue adsorption, *Dyes and Pigments* 75 (2007) 263–272.
- [30] Q.S. Liu, T. Zheng, N. Li, P. Wang, G. Abulikemu, Modification of bamboo-based activated carbon using microwave radiation and its effects on the adsorption of methylene blue, *Applied Surface Science* 256 (2010) 3309–3315.
- [31] P.J. Lu, H.C. Lin, W.T. Yu, J.M. Chern, Chemical regeneration of activated carbon used for dye adsorption, *Journal of the Taiwan Institute of Chemical Engineers* 42 (2011) 305–311.
- [32] M.K. Purkait, A. Maiti, S. DasGupta, S. De, Removal of Congo Red using activated carbon and its regeneration, *Journal of Hazardous Materials* 145 (2007) 287–295.